HHS Public Access

Author manuscript

*J Neurochem*. Author manuscript; available in PMC 2016 July 01.

Published in final edited form as:

*J Neurochem*. 2015 July ; 134(1): 56–65. doi:10.1111/jnc.13104.

# Methamphetamine acutely inhibits voltage-gated calcium channels but chronically upregulates L-type channels

**M.A. Andres, Ph.D.**[1,‡], **I.M. Cooke, Ph.D.**[1,1a], **F.P. Bellinger, Ph.D.**[2], **M.J. Berry, Ph.D.**[2], **M. Zaporteza, Ph.D.**[1], **R.H. Rueli**[2], **S.M. Barayuga**[2], and **L. Chang, M.D.**[3]

[1]Bekesy Laboratory of Neurobiology, Pacific Biosciences Research Center, University of Hawaii, Honolulu, HI 96822

[1a]Department of Biology, University of Hawaii, Honolulu, HI 96822

[2]Department of Cell and Molecular Biology, John A. Burns School of Medicine, University of Hawaii, Honolulu, HI 96813

[3]Department of Medicine, John A. Burns School of Medicine, University of Hawaii, Honolulu, HI 96813

## Abstract

In neurons, calcium ($Ca^{2+}$) channels regulate a wide variety of functions ranging from synaptic transmission to gene expression. They also induce neuroplastic changes that alter gene expression following psychostimulant administration. $Ca^{2+}$ channel blockers have been considered as potential therapeutic agents for the treatment of methamphetamine (METH) dependence because of their ability to reduce drug craving among METH users. Here, we studied the effects of METH exposure on voltage-gated $Ca^{2+}$ channels using SH-SY5Y cells as a model of dopaminergic neurons. We found that METH has different short- and long-term effects. A short-term effect involves immediate (<5 min) direct inhibition of $Ca^{2+}$ ion movements through $Ca^{2+}$ channels. Longer exposure to METH (20 min or 48 hr) selectively upregulates the expression of only the *CACNA1C* gene, thus increasing the number of L-type $Ca^{2+}$ channels. This upregulation of *CACNA1C* is associated with the expression of the CREB (cAMP responsive element binding protein), a known regulator of *CACNA1C* gene expression, and the *MYC* gene, which encodes a transcription factor that putatively binds to a site proximal to the *CACNA1C* gene transcription initiation site. The short-term inhibition of $Ca^{2+}$ ion movement and later, the upregulation of $Ca^{2+}$ channel gene expression together suggest the operation of CREB- and C-MYC-mediated mechanisms to compensate for $Ca^{2+}$ channel inhibition by METH. Increased $Ca^{2+}$ current density and subsequent increased intracellular $Ca^{2+}$ may contribute to the neurodegeneration accompanying chronic METH abuse.

### Keywords

Methamphetamine; calcium signaling; calcium channel; CACNA1C; CACNA1B; MYC

[‡]Corresponding author: Marilou A. Andres, Ph.D., Bekesy Laboratory of Neurobiology, Pacific Biosciences Research Center, 1993 East-West Road, Honolulu, HI 96822, (Phone) 808-956-8036; (Fax) 808-956-6984, marilou@pbrc.hawaii.edu.

The authors have no conflicts of interest to declare.

## INTRODUCTION

Calcium ions ($Ca^{2+}$) are involved in regulating intracellular signaling in response to psychostimulants (White & Kalivas 1998, Wolf 1998, Licata & Pierce 2003). In neurons and other excitable cells, entry of extracellular $Ca^{2+}$ ions is mediated by the activation of voltage-gated $Ca^{2+}$ channels (VGCC) (Thayer *et al.* 1986, Sanna *et al.* 1986) in response to cell membrane depolarization. Of the various types of VGCCs that are found in neurons, the N- and P/Q-types are expressed in axonal boutons (Hardingham *et al.* 1998) and the L-type channels are found on axons (Tippens *et al.* 2008) and dendrites and in presynaptic terminals where they mediate release of neuromodulators as well as $Ca^{2+}$-dependent gene expression (Hardingham et al. 1998).

Studies show that $Ca^{2+}$ entry through VGCCs contribute to the mechanism underlying neurochemical and behavioral changes in response to psychostimulant exposure (Pierce & Kalivas 1997, Pierce *et al.* 1998, Licata *et al.* 2000, Pliakas *et al.* 2001). While blocking N-methyl-D-aspartate (NMDA) receptors inhibits both acute and chronic psychostimulant responses (Vezina & Queen 2000, Karler *et al.* 1989), blocking L-type $Ca^{2+}$ channels only inhibits chronic but not acute psychostimulant- induced neurochemical and behavioral changes (Karler *et al.* 1991, Pierce & Kalivas 1997, Pierce et al. 1998). L-type $Ca^{2+}$ channels mediate long-term neuronal plasticity and induce persistent neuroadaptations in the ventral tegmental area (VTA) of the brain (Bito *et al.* 1996, Deisseroth *et al.* 2003). The L-type $Ca^{2+}$ channels also play a role in amphetamine-mediated ERK1/2 phosphorylation in the VTA (Rajadhyaksha *et al.* 2004) during chronic but not acute amphetamine treatments in rats. Consistent with these observations, chronic amphetamine treatment is associated with the upregulation of the L-type $Ca^{2+}$ channel transcript and protein.

According to the World Drug Report in 2012, ampthetamine-type stimulants, most commonly methamphetamine (METH), are the second most used illicit drug in the world (http://www.who.int/substance_abuse/facts/psychoactives/en/). To date there is no known effective pharmacological therapy for METH dependence. Nifedipine, an L-type $Ca^{2+}$ channel blocker, dose- dependently reduces the development of METH's rewarding effect in mice (Shibasaki *et al.* 2010). $Ca^{2+}$ channel blockers were also considered as potential therapeutic agents for the treatment of METH dependence because of their ability to reduce drug craving among METH users (Johnson *et al.* 1999) and reduce some methamphetamine-induced positive subjective and reinforcing effects (Johnson *et al.* 2005). However, more research is needed to evaluate and delineate the mechanism by which $Ca^{2+}$ channels mediate the addictive properties of METH.

The human SH-SY5Y cell line has been used as a dopaminergic neuron model for studies investigating the effects of METH (Chetsawang *et al.* 2012, Suwanjang *et al.* 2010). Two subtypes of the voltage-gated $Ca^{2+}$ channels (L-type and N-type) have been functionally characterized and identified in this cell line (Reuveny & Narahashi 1993). In this study, we investigated the effects of METH on the voltage-gated $Ca^{2+}$ channels of human SH-SY5Y cells. We hypothesized that METH would alter $Ca^{2+}$ channel function and gene expression patterns. We found that METH acutely (in minutes) inhibits inward voltage-gated $Ca^{2+}$

current, but with long-exposure (in as early as 20 min and in days) METH augmented expression of $Ca^{2+}$ channels.

## METHODS

### Cell Culture

Undifferentiated adherent SH-SY5Y cells were grown in Dulbecco's Modified Eagle Medium (Thermo Scientific, Rockford, IL) with 10% FBS (Thermo Scientific, Rockford, IL), 2 mM L-alanyl-L-glutamine (Sigma-Aldrich, Missouri, USA), and 1x Penicillin Streptomycin (Thermo Scientific, Rockford, IL) and were maintained under 37°C and 5% $CO_2$ conditions. Cells were then differentiated, as previously described (Barayuga *et al.* 2013), with Neurobasal Medium that was supplemented with 2 mM L-alanyl-L-glutamine, 1X Penicillin Streptomycin and 1x B-27 Serum-Free Supplement (Life Technologies, New York, USA). Retinoic acid in the B-27 supplement induced differentiation.

### Electrophysiological measurements

For electrophysiology, SH-SY5Y cells were plated sparsely on glass coverslips 24 hours prior to recording. Whole-cell patch clamp recordings were conducted using an EPC-9 amplifier. Data were acquired using PatchMaster software (HEKA, Germany). Electrodes with resistances of 2-3 MΩ were pulled from capillaries made of borosilicate glass (King Precision Glass Inc., California) using a Sutter P-97 Puller (Sutter Instrument Co., California). The electrode solution consisted of (in mM): 130 CsCl, 2 $MgCl_2$, 10 $CaCl_2$, 10 HEPES, 10 Glucose with pH of 7.2 and osmolarity of ~300 mOsm. Whole-cell currents were sampled every 80μs. Currents were evoked by depolarizing voltage steps as described in the figure legends. Cells were bathed in recording solutions consisting of (in mM): 130 NMDG, 2 $MgCl_2$, 10 $CaCl_2$, 10 HEPES, and 10 Glucose with pH of 7.4 and an osmolality of ~300 mOsm. Toxin, blocker, or METH, at concentrations indicated in the text, was added to the external solutions. In the recording chamber, fast solution changes are achieved using a digitally controlled microperfusion system SmartSquirt® Micro-Perfusion System (Automate Scientific, Inc., California). Only cells being recorded were constantly perfused with the control external solution and solution containing toxin, blocker, or METH.

### METH treatments

Differentiated SH-SY5Y cells, maintained in supplemented Neurobasal Medium, were treated with the indicated amount of methamphetamine hydrochloride (Sigma-Aldrich, Missouri, USA). Supernatants were assayed for cell viability (below). For some experiments, cells were also treated with both METH and SCH 23390 as indicated. Cells were harvested for RNA extraction and qPCR assays.

### Cell proliferation/viability assay

Cell viability was evaluated using CellTiter 96® $AQ_{ueous}$ Non-Radioactive Cell Proliferation Assay (Promega, Wisconsin, USA) per manufacturer's protocol. This assay is a colorimetric method for quantifying cell proliferation based on the conversion of 3-(4,5-dimethylthiazol-2-yl)-5-(3-carboxymethoxyphenyl)-2-(4-sulfophenyl)-2H-tetrazolium (MTS) into formazan by dehydrogenase enzymes that are found in metabolically active

cells. Briefly, METH-treated and untreated cells (negative control) were exposed to the recommended amount of phenazine methosulfate (PMS) and MTS solution, and then incubated for 4 hours at 37°C and 5% $CO_2$ conditions. Then, absorbance of the formazan was read at 490nm directly from 96-well assay plates using a plate reader. The amount of formazan product is directly proportional to the number of live cells in the culture.

### RNA extraction and cDNA synthesis

Treated and untreated control cells were pelleted by centrifugation and washed with PBS (Phosphate Buffered Saline), trypsinized, and resuspended in B27-supplemented Neurobasal medium. Cells were then centrifuged and the resulting cell pellet was then washed with PBS. RNA samples were extracted using an RNeasy Mini Kit (QIAGEN Inc., California, USA) that included an additional step to eliminate the genomic DNA. RNA sample concentration and purity were then determined using a NanoDrop 1000 (Thermo Fisher Scientific Inc., Delaware, USA). The first strand of cDNA was synthesized from 1μg of total RNA template using $RT^2$ First Strand Synthesis (QIAGEN Inc., California, USA).

### PCR array and real-time PCR

In a 96-well PCR array plate, the cDNA sample and the specific primer pairs were added to the $RT^2$ SYBR Green PCR Master Mix (QIAGEN Inc., California, USA). We initially screened $Ca^{2+}$ channel gene expression using PCR array PAHS-036 (Qiagen Inc., California, USA) to assess the presence of 84 ion channel genes and receptors in our samples. Subsequently, to quantify the expression levels of $Ca^{2+}$ channel genes, we used predesigned PrimeTime® qPCR specific primers (Integrated DNA Technologies, Iowa, US) for CACNA1B (primer 1: 5'-GGTCTCTGGTGGTTTTGTTCT -3'; primer 2: 5'-AGGAGATTTCCGTTGTGTGG -3'), CACNA1C (primer 1: 5'-GTCCGCTTCCAGATCTTCTTG-3'; primer 2: 5'-TGTTCAATGCCACCCTGTT -3'), *CACNA1D (primer 1: 5'-GGAAGTCTGGTGCCTCTTG*- 3'; primer 2: 5'-GCTCAATAAATGTTCGTGGATGA-3') and the transcription factor genes, MYC (primer 1: 5'-CGTAGTCGAGGTCATAGTTCC-3'; primer 2: 5'-GCTGCTTAGACGCTGGATT-3') and CREB1 (primer 1: 5'-ATAAAACTCCAGCGAGATCCG-3'; primer 2: 5'-GTTACAGCTGCATCTCCACT-3'), and the housekeeping gene HPRT1(primer 1: 5'-AGGTATGCAAAATAAATCAAGGTCAT -3'; primer 2: 5'-TCCTCCTGAGCAGTCAGC -3') and reran the real-time PCR for each experiment in triplicate or quadruplicate.

### Gene Expression (Gene fold) Analysis

Cycle threshold values (C(t)) for *CREB1*, *MYC*, *CACNA1B*, *CACNA1C*, *CACNA1D* and *HPRT1* for each experimental sample were determined from the real-time PCR runs. Relative mRNA levels were determined by first correcting C(t) values using the formula: ΔC(t) sample = C(t) gene of interest – C(t) HPRT gene. The average corrected C(t) values for the untreated cells were then determined. The fold change level for each sample was calculated using the formula: ΔΔC(t) METH-treated sample = ΔC(t) METH-treated sample - average corrected C(t) untreated-cells.

### Statistical Analysis

We compared the METH-treated and untreated groups for the level of gene expression, inhibition of $Ca^{2+}$ flux and cell viability either by t-test or by ANOVA. These variables are reported as group mean values ± SD. Group comparisons with $P<0.05$ were considered statistically significant. Pearson correlation was used to examine the relationship between the expression of *CACNA1C* and *MYC* genes. Multiple linear regression was used to examine interactions between *CACNA1C*, *CREB/C-MYC*, and METH status.

## RESULTS

First, we determined the expression of genes coding for different $Ca^{2+}$ channel subtypes in SH-SY5Y cells. Of the six subtypes (*CACNA1A*, *CACNA1B*, *CACNA1C*, *CACNA1D*, *CACNA1H*, and *CACNA1S)* assessed, only three $Ca^{2+}$ channel genes, *CACNA1B*, *CACNA1C*, and *CACNA1D*, showed detectable expression levels as pre-screened using catalogued PCR arrays. In Figure 1, real-time qPCR analysis indicated that while the *CACNA1B* gene showed significantly lower expression levels compared to *CACNA1C* and *CACN1D* genes (Normalized Ct ANOVA, $p=0.005$), the expression levels of *CACNA1C* and *CACN1D* genes did not differ significantly from each other ($p=0.28$). *CACNA1C* and *CACNA1D* encode for the L-type $Ca^{2+}$ channel (Karnabi *et al.* 2009) while *CACNA1B* encodes for the N-type $Ca^{2+}$ channel (Miyamoto *et al.* 2009).

These $Ca^{2+}$ channel genes expressed functional proteins based on their sensitivities to specific blockers when assessed using electrophysiological recordings. As shown in Figure 1B, whole-cell patch clamp recordings demonstrate that the inward $Ca^{2+}$ currents are inhibited by ω-conotoxin MVIIC (1 μM), a peptide neurotoxin which targets N-type $Ca^{2+}$ channels. Inhibition was maximal within 3-5 minutes. The average inhibition at this dose was 24.4±19.2SD%. Figure 1C shows that these $Ca^{2+}$ currents are also inhibited by nifedipine (2μM), a selective blocker of L-type $Ca^{2+}$ channels. Inhibition was maximal within 2 minutes. Current was reduced by 22±19SD%. Note that the recording solution used in this and the following recordings was designed to isolate voltage-gated $Ca^{2+}$ currents and the doses used for the conotoxin and nifedipine treatments are non-saturating, partially inhibiting only a fraction of the N-type and L-type $Ca^{2+}$ channels present (Shen *et al.* 2000, McDonough *et al.* 1996).

We assessed the effects of 24- and 48-hour METH treatments over a range of doses (7.8μM-1mM) on cell viability using a cell viability assay. These exposure times replicate the human condition of a METH user “binging” for 2 days. Figure 2 demonstrates a dose-dependent reduction of cell survival at concentrations ranging from 125μM to 1mM METH after 48 hours of exposure. Higher concentrations were required to reduce viability with a shorter, 24-hour treatment. Nifedipine (2.4μM) had no effect on cell viability.

The patch clamp recordings reproduced in Figure 3A shows that a high dose of METH (1mM) completely suppressed voltage-gated $Ca^{2+}$ channels. This inhibition occurred within 1-2 minutes of METH exposure. Figures 3A and 3B further demonstrate that the inhibition by METH is reversible upon washout with control solutions. Since METH is found in the human body fluid and tissue ranging from 0.1μM (Melega*et al.* 2007) to 138μM (Moriya &

Hashimoto 2002), we tested whether METH had any effects on $Ca^{2+}$ channels within this range. We observed that 50μM METH also reduced $Ca^{2+}$ currents by 24 ± 17SD% in <5 minutes (Figure 3c). These data show that one of METH's short-term effects is to inhibit $Ca^{2+}$ channel activity.

Next, we evaluated the long-term effect of METH on $Ca^{2+}$ channel gene expression. We exposed SHSY5Y cells to 50 μM METH for 48 hours and found that METH has a significant effect on the expression levels of *CACNA1C* mRNA ($p$=0.031) encoding for L-type channel protein but not on *CACNA1B* (N-type) and *CACNA1D* (L-type) mRNAs (Figure 4A). We tested whether this upregulation of the *CACNA1C* gene translated into the formation of functional channel proteins as early as a few hours after METH exposure. Indeed, patch clamp recordings of METH-treated cells confirmed this; Figure 4B shows that METH-treated cells, recorded as early as 3 hrs post-exposure, exhibited significantly greater amplitude of whole-cell inward current density (current/membrane capacitance). We used the current density to quantify the $Ca^{2+}$ channel density based on functional activities of $Ca^{2+}$ channels that are expressed in the entire cell membrane.

We examined whether METH affected the expression of the transcription factor genes, *CREB1* and *MYC*. *CREB1* encodes for CRE-binding protein (CREB), a transcription factor that binds to cAMP response element (CRE) in the promoter region of the *CACNA1C* gene to regulate channel expression (Tsai *et al.* 2007). *MYC* encodes the transcription factor C-MYC that putatively binds to a site proximal to the transcription initiation site of the *CACNA1C* gene. We found that exposure to METH significantly increased the expression of *CREB1* (Figure 5A, left panel). We also found the *CACNA1C* expression was positively associated with *CREB1* expression in the presence of METH but was inversely correlated in the absence of METH (Figure 5A, right panel). Although we did not see any difference in the expression levels of *C-MYC* between untreated- and METH-treated cells (Figure 5B, left panel), we found that the expression levels of *CACNA1C* mRNA are correlated with that of the *C-MYC* transcription factor gene (Figure 5B, right panel: overall r=0.7, p=0.0002), with no significant difference between the slopes for METH-treated and non-treated cells (ANCOVA $p$=0.5).

We also investigated whether activation of the dopamine D1 receptors (D1DR) may be involved in the upregulation of *CACNA1C* as METH increases extracellular dopamine to promote activation of the D1DR receptors. We blocked D1DRs with the selective antagonist SCH 23390 in the presence of METH. As shown in Figure 6A, 10μM SCH 233390 in the presence of 50μM METH reduced *CACNA1C* expression to levels comparable to control cells (METH-). However, treatment with SKF 82958, a full dopamine D1 receptor agonist, did not increase *CACNA1C* expression, as expression levels remained comparable to untreated control cells. This suggests that the upregulation of *CACNA1C* expression involves not only the activation of the D1DRs but may also require the presence of METH. We also investigated how activation and suppression of the D1DRs affects the two transcription factor genes. While *C-MYC* expression was unaffected by SKF 82958 and SCH 23390 (data not shown), Figure 6B shows that 10μM SCH 23390 in the presence of 50μM METH suppressed *CREB1* expression. In contrast, treatment with the D1DR agonist SKF 82958 upregulated *CREB1* expression to levels that were significantly higher than those of

the control, untreated cells. Hence, together, these data indicate that the upregulation of the *CACNA1C* calcium channel gene requires a combination of enhanced *CREB1* expression and the presence of METH (Figures 6A and 6B). In contrast, a combination of enhanced *CREB1* expression and activation of D1DR by its agonist is not sufficient to upregulate *CACNA1C* expression, suggesting that additional factors other than *CREB1* are necessary to increase *CACNA1C* expression.

## DISCUSSION

We report our new, novel finding that METH directly and immediately affects $Ca^{2+}$ channels in the cultured SH-SY5Y model of dopaminergic neurons. Our data shows that METH, at a concentration found in the blood and tissue of METH users (50 μM), inhibits inward $Ca^{2+}$ movements through voltage-gated $Ca^{2+}$ channels. Inhibition of voltage-gated $Ca^{2+}$ current by inhibitors specific for N-type and L-type $Ca^{2+}$ channels, together with gene-expression data, show that both of these channel types are present in the SH-SY5Y dopaminergic neurons. Because a high concentration (1mM) of METH completely, but reversibly, suppressed inward $Ca^{2+}$ currents, we conclude that METH inhibits both types of $Ca^{2+}$ channels.

Our study also examined the effects of longer METH exposure (20 min and 48 hrs) on VGCCs and on gene expression levels for N-type and L-type $Ca^{2+}$ channels. Inward current density (recorded in standard saline) was significantly increased, as would be expected from the observed increase in the expression levels of the gene encoding the L-type $Ca^{2+}$ channels. Expression levels for the N-type $Ca^{2+}$ channels were not changed.

Numerous studies have investigated the effects of amphetamine, a by-product of METH. It is plausible that METH and amphetamine affect similar, if not the same, pathways. Specifically, acute amphetamine administration leads to glutamate release via presynaptic D1 receptor activation and to the release of dopamine in the ventral tegmental area (VTA ) neurons (Licata & Pierce 2003). Glutamate (Glu) then activates AMPA -type Glu receptors, which subsequently depolarize the cell membrane and activate NMDA-type Glu receptors in VTA neurons. In turn, the $Ca^{2+}$-second messenger pathway is activated through calmodulin (CaM) and subsequently through the calmodulin kinase pathway. These then lead to the phosphorylation of CREB (pCREB) and the activation of gene expression. It is thought that this pathway is responsible for the gene expression changes that underlie the long-lasting molecular and behavioral changes associated with amphetamine abuse. Consonant with our observations, recent studies demonstrate that chronic but not acute amphetamine administration increases Cav1.2 mRNA (*CACNA1C*) and protein (i.e. the L-type $Ca^{2+}$ channel), suggesting that L-type $Ca^{2+}$ channels are important in inducing persistent neuroadaptations in the VTA (Rajadhyaksha et al. 2004, Bito et al. 1996, Deisseroth et al. 2003).

Our finding of long-term or chronic effects of METH on *CACNA1C* gene expression, which encodes for the L-type $Ca^{2+}$ channel, provides further evidence for the mechanism of METH-induced neuroadaptation. These findings may also explain observations that METH enhances intracellular $Ca^{2+}$ concentrations and oscillations in neurons (Uramura *et al.* 2000)

and elicits bursts of action potentials (Melega et al. 2007). In non-neuronal cells (kidney cells expressing human dopamine transporters), METH elevates intracellular $Ca^{2+}$ concentration, but this increase is attributed to $Ca^{2+}$ released from intracellular $Ca^{2+}$ stores (Goodwin *et al.* 2009). However, it is not known whether METH has any direct effects on $Ca^{2+}$ release from intracellular stores in neurons. Only one study demonstrated that METH upregulates the expression of ryanodine receptor mRNA and protein (a component of the ER $Ca^{2+}$ release channel) through the dopamine D1 receptor signaling system in midbrain neurons and cerebral cortical neurons (Kurokawa *et al.* 2011). Further, the long-term or chronic effect of an upregulation of the L-type $Ca^{2+}$ channel gene *CACNA1C* by METH has possible toxic effects. We postulate that the upregulation of these channels underlies the increases in $[Ca^{2+}]_i$ in dopaminergic neurons, as observed by others (Uramura et al. 2000), and leads to neuronal death due to toxicity (Barayuga et al. 2013). Cadet and colleagues have proposed that METH promotes $Ca^{2+}$-mediated neurotoxicity (Cadet *et al.* 2003). Our dose-dependent decreases in cell viability with higher concentrations of METH supports this view.

To determine the mechanism that may underlie the upregulation of L-type $Ca^{2+}$ channels, we assessed the role of transcription factors in regulating $Ca^{2+}$ channel gene expression changes during METH exposure. We evaluated the expression levels of two transcription factors. CREB has previously been shown to bind to the CRE DNA sequences in the promoter region of the *CACNA1C* gene to regulate channel transcription (Tsai et al. 2007). CREB also mediates transcription of genes encoding other transcription factors, as found in a study of METH self-administration in rats (Krasnova *et al.* 2013). Consistent with other findings (Cadet *et al.* 2014, Han *et al.* 2011), we found that CREB is elevated under METH and is positively correlated with *CACNA1C* L-type $Ca^{2+}$ channel expression in the presence of METH but inversely correlated with L-type $Ca^{2+}$ channel gene expression in the absence of METH. Our data also shows that the dopamine D1 receptor signaling pathway may modulate *CACNA1C* expression via CREB and that this is dependent upon the presence of METH. Hence, these findings suggest that CREB may contribute to the upregulation of *CACNA1C* in the presence of METH but not in the absence of METH. Further, we speculate that *CACNA1C* may potentially be one of the genes that are turned on by the CREB transcription factor during METH-induced neuroadaptation.

C-MYC has been shown to be responsive to METH (Thiriet *et al.* 2001). Its binding site is located upstream of the *CACNA1C* gene transcription initiation site, based on information from the UCSC Genome Browser. Interestingly, the levels of *C-MYC* expression were not any different between untreated- and 48 hr METH treated-cells. Our findings are consistent with a prior study in mouse brain that found METH administration increased mRNA and protein levels of *C-MYC* in the dopaminergic region of the brain (striatum) in a biphasic pattern, after 20 min and again at 4 hr post-METH exposure, but returning to control levels after 2 days (Thiriet et al. 2001). Since we did not measure these levels at the earlier time points, we might have missed detecting the earlier elevation of *C-MYC* expression in these human-derived cells. We also found a positive correlation between *C-MYC*'s expression levels and *CACNA1C* expression levels, with or without METH treatments. These suggest that C-MYC may be involved in regulating basal transcription of L-type channels in both

untreated and METH-treated cells, but some additional factors (such as CREB) are involved in further enhancing the expression of the *CACNA1C* gene in the presence of METH. However, we found that D1DR activation had no effect on CMYC. Together, these data suggest that CREB and C-MYC transcription factors have differing roles in enhancing and regulating the expression of the L-type $Ca^{2+}$ channel. More work is needed to definitively demonstrate that *C-MYC* is regulating the expression of *CACNA1C* during METH exposure.

Another potential mechanism by which L-type $Ca^{2+}$ channel gene expression could be altered by METH is through auto-regulation. The L-type $Ca^{2+}$ channel has been shown to have the capacity to self-regulate (Satin *et al.* 2011) such that a chronic blockade of L-type $Ca^{2+}$ channel activities promotes the up-regulation of the channel protein (Schroder *et al.* 2007). In this self-regulating mechanism, a segment of the L-type $Ca^{2+}$ channel protein, the distal C-terminus (DCT), translocates to the nucleus (Gomez-Ospina*et al.* 2006). This proteolytically cleaved DCT fragment links the signal from the L-type $Ca^{2+}$ channel activities directly to a change in transcription in the nucleus, essentially serving as a "mobile" transcription factor. In neurons, the translocated DCT fragment regulates transcription of other ion channel genes including an up-regulation of connexin 31.1 (*gjb5*) and down-regulation of the TRPV4 channel (*trpv4*), the $Ca^{2+}$-activated SK3 potassium channel (*kcnn3*), and the $Na^{+}$/ $Ca^{2+}$ exchanger (*scl8a1*) (Gomez-Ospina et al. 2006). Our findings are consistent with the DCT activation mechanism. We suggest that when METH inhibits $Ca^{2+}$ channel activity during acute exposure, the reduction of $Ca^{2+}$ signal and reduction in intracellular $Ca^{2+}$ load leads to the upregulation of L-type $Ca^{2+}$ channel expression, perhaps by means of this mobile transcription factor mechanism. However, we have found no study investigating whether METH promotes the cleavage of a channel fragment that serves as a mobile transcription factor during chronic exposure to METH. Additionally, while METH was reported to inhibit L-type $Ca^{2+}$ channels in cardiac cells (Liang *et al.* 2010), no prior study investigated the possible blockade of L-type $Ca^{2+}$ channels by METH in neurons, or how this might mediate neuroadaptation during chronic METH use. Our data provides a starting point for examining the mechanism linking functional signals from $Ca^{2+}$ channels to gene expression changes during short and long-term METH exposure.

In summary, Figure 7 depicts our proposed working model. Acutely (<5 min), METH directly inhibits voltage-gated N-type and L-type $Ca^{2+}$ channels. During chronic exposure (>20min), cells compensate by elevating *CACNA1C* L-type channel gene expression. The long-term changes in channel expression are mediated by transcription factors C-MYC and CREB. Furthermore, regulation of CREB expression is also possible through activation of the D1DR transduction pathway as a result of an increase in dopamine levels due to METH-induced dysfunction of the dopamine transporters at the presynaptic terminal However, activation of the D1DRs and upregulation of CREB are not sufficient to increase expression of L-type calcium channels. In contrast, blocking the D1DR with its antagonist even in the presence of METH leads to reduction in CREB expression and significant reduction of L-type channel expression (relative to METH-treated levels). According to this model, the increased calcium channel density accompanying chronic METH exposure leads to higher

intracellular $Ca^{2+}$ load and subsequently to $Ca^{2+}$-mediated neurotoxicity and neurodegeneration.

## ACKNOWLEDGEMENTS

This work was supported by research grants (5R24DA027318, 5G12MD007601, K24DA16170 and 1R03DA033904) from the National Institutes of Health.

## Abbreviations

| | |
|---|---|
| **METH** | Methamphetamine |
| **$Ca^{2+}$** | calcium |
| **DCT** | distal C-terminus |
| **NMDA** | N-methyl-D-aspartate |
| **PBS** | Phosphate Buffered Saline |
| **MTS** | 3-(4,5-dimethylthiazol-2-yl)-5-(3-carboxymethoxyphenyl)-2-(4-sulfophenyl)-2H-tetrazolium |
| **PMS** | phenazine methosulfate |
| **VGCC** | voltage-gated calcium channel |
| **CREB** | cAMP responsive element binding protein |
| **NMDA** | N-methyl-D-aspartate |
| **VTA** | ventral tegmental area |
| **AMPA** | α-Amino-3-hydroxy-5-methyl-4-isoxazolepropionic acid |
| **ERK** | extracellular signal-regulated protein kinase |
| **MYC** | Myelocytomatosis oncogene cellular homolog |
| **NMDG** | N-methyl-D-glucamine |
| **FBS** | Fetal Bovine Serum |

## REFERENCES

Barayuga SM, Pang X, Andres MA, Panee J, Bellinger FP. Methamphetamine decreases levels of glutathione peroxidases 1 and 4 in SH-SY5Y neuronal cells: protective effects of selenium. Neurotoxicology. 2013; 37:240–246. [PubMed: 23721877]

Bito H, Deisseroth K, Tsien RW. CREB phosphorylation and dephosphorylation: a Ca(2+)- and stimulus duration-dependent switch for hippocampal gene expression. Cell. 1996; 87:1203–1214. [PubMed: 8980227]

Cadet JL, Brannock C, Jayanthi S, Krasnova IN. Transcriptional and Epigenetic Substrates of Methamphetamine Addiction and Withdrawal: Evidence from a Long-Access Self-Administration Model in the Rat. Molecular neurobiology. 2014

Cadet JL, Jayanthi S, Deng X. Speed kills: cellular and molecular bases of methamphetamine-induced nerve terminal degeneration and neuronal apoptosis. FASEB journal : official publication of the Federation of American Societies for Experimental Biology. 2003; 17:1775–1788. [PubMed: 14519657]

Chetsawang J, Suwanjang W, Pirompul N, Govitrapong P, Chetsawang B. Calpastatin reduces methamphetamine-induced induction in c-Jun phosphorylation, Bax and cell death in neuroblastoma SH-SY5Y cells. Neuroscience letters. 2012; 506:7–11. [PubMed: 22027180]

Deisseroth K, Mermelstein PG, Xia H, Tsien RW. Signaling from synapse to nucleus: the logic behind the mechanisms. Current opinion in neurobiology. 2003; 13:354–365. [PubMed: 12850221]

Gomez-Ospina N, Tsuruta F, Barreto-Chang O, Hu L, Dolmetsch R. The C terminus of the L-type voltage-gated calcium channel Ca(V)1.2 encodes a transcription factor. Cell. 2006; 127:591–606. [PubMed: 17081980]

Goodwin JS, Larson GA, Swant J, Sen N, Javitch JA, Zahniser NR, De Felice LJ, Khoshbouei H. Amphetamine and methamphetamine differentially affect dopamine transporters in vitro and in vivo. The Journal of biological chemistry. 2009; 284:2978–2989. [PubMed: 19047053]

Han W, Takamatsu Y, Yamamoto H, Kasai S, Endo S, Shirao T, Kojima N, Ikeda K. Inhibitory role of inducible cAMP early repressor (ICER) in methamphetamine-induced locomotor sensitization. PloS one. 2011; 6:e21637. [PubMed: 21738744]

Hardingham GE, Cruzalegui FH, Chawla S, Bading H. Mechanisms controlling gene expression by nuclear calcium signals. Cell calcium. 1998; 23:131–134. [PubMed: 9601608]

Johnson BA, Ait-Daoud N, Bordnick PS. Effects of isradipine, a dihydropyridine-class calcium channel antagonist, on d-methamphetamine-induced reduction in hunger. Progress in neuro-psychopharmacology & biological psychiatry. 1999; 23:1227–1234. [PubMed: 10581644]

Johnson BA, Roache JD, Ait-Daoud N, Wallace CL, Wells LT, Wang Y, Dawes MA. Effects of isradipine on cocaine-induced changes in cognitive performance in recently abstinent cocaine-dependent individuals. The international journal of neuropsychopharmacology / official scientific journal of the Collegium Internationale Neuropsychopharmacologicum. 2005; 8:549–556.

Karler R, Calder LD, Chaudhry IA, Turkanis SA. Blockade of “reverse tolerance” to cocaine and amphetamine by MK-801. Life sciences. 1989; 45:599–606. [PubMed: 2671566]

Karler R, Calder LD, Turkanis SA. Calcium channel blockers and excitatory amino acids. Brain research. 1991; 551:331–333. [PubMed: 1913163]

Karnabi E, Qu Y, Mancarella S, Yue Y, Wadgaonkar R, Boutjdir M. Silencing of Cav1.2 gene in neonatal cardiomyocytes by lentiviral delivered shRNA. Biochemical and biophysical research communications. 2009; 384:409–414. [PubMed: 19422800]

Krasnova IN, Chiflikyan M, Justinova Z, et al. CREB phosphorylation regulates striatal transcriptional responses in the self-administration model of methamphetamine addiction in the rat. Neurobiology of disease. 2013; 58:132–143. [PubMed: 23726845]

Kurokawa K, Mizuno K, Kiyokage E, Shibasaki M, Toida K, Ohkuma S. Dopamine D1 receptor signaling system regulates ryanodine receptor expression after intermittent exposure to methamphetamine in primary cultures of midbrain and cerebral cortical neurons. Journal of neurochemistry. 2011; 118:773–783. [PubMed: 21707617]

Liang R, Zhou Y, Wu F, Zhou C, Zhao X, Zhang M, Tian X, Zhu B. Effect of methamphetamine on potassium and L-type calcium currents in rat ventricular myocytes. Toxicology mechanisms and methods. 2010; 20:458–465. [PubMed: 20608758]

Licata SC, Freeman AY, Pierce-Bancroft AF, Pierce RC. Repeated stimulation of L-type calcium channels in the rat ventral tegmental area mimics the initiation of behavioral sensitization to cocaine. Psychopharmacology. 2000; 152:110–118. [PubMed: 11041323]

Licata SC, Pierce RC. The roles of calcium/calmodulin-dependent and Ras/mitogen-activated protein kinases in the development of psychostimulant-induced behavioral sensitization. Journal of neurochemistry. 2003; 85:14–22. [PubMed: 12641723]

McDonough SI, Swartz KJ, Mintz IM, Boland LM, Bean BP. Inhibition of calcium channels in rat central and peripheral neurons by omega-conotoxin MVIIC. The Journal of neuroscience : the official journal of the Society for Neuroscience. 1996; 16:2612–2623. [PubMed: 8786437]

Melega WP, Cho AK, Harvey D, Lacan G. Methamphetamine blood concentrations in human abusers: application to pharmacokinetic modeling. Synapse. 2007; 61:216–220. [PubMed: 17230548]

Miyamoto N, Namiki K, Tokuhara N, Uesugi M, Takahashi E, Kuromitsu J, Kasuya Y. The utilization of gene targeting models during in preclinical study of drug discovery process--example of

phenotypic and functional analysis of Cacna1beta gene product. Current pharmaceutical biotechnology. 2009; 10:261–267. [PubMed: 19199960]

Moriya F, Hashimoto Y. A case of fatal hemorrhage in the cerebral ventricles following intravenous use of methamphetamine. Forensic science international. 2002; 129:104–109. [PubMed: 12243878]

Pierce RC, Kalivas PW. Repeated cocaine modifies the mechanism by which amphetamine releases dopamine. The Journal of neuroscience : the official journal of the Society for Neuroscience. 1997; 17:3254–3261. [PubMed: 9096158]

Pierce RC, Quick EA, Reeder DC, Morgan ZR, Kalivas PW. Calcium-mediated second messengers modulate the expression of behavioral sensitization to cocaine. The Journal of pharmacology and experimental therapeutics. 1998; 286:1171–1176. [PubMed: 9732375]

Pliakas AM, Carlson RR, Neve RL, Konradi C, Nestler EJ, Carlezon WA Jr. Altered responsiveness to cocaine and increased immobility in the forced swim test associated with elevated cAMP response element-binding protein expression in nucleus accumbens. The Journal of neuroscience : the official journal of the Society for Neuroscience. 2001; 21:7397–7403. [PubMed: 11549750]

Rajadhyaksha A, Husson I, Satpute SS, Kuppenbender KD, Ren JQ, Guerriero RM, Standaert DG, Kosofsky BE. L-type Ca2+ channels mediate adaptation of extracellular signal-regulated kinase 1/2 phosphorylation in the ventral tegmental area after chronic amphetamine treatment. The Journal of neuroscience : the official journal of the Society for Neuroscience. 2004; 24:7464–7476. [PubMed: 15329393]

Reuveny E, Narahashi T. Two types of high voltage-activated calcium channels in SH-SY5Y human neuroblastoma cells. Brain research. 1993; 603:64–73. [PubMed: 7680940]

Sanna E, Head GA, Hanbauer I. Evidence for a selective localization of voltage-sensitive Ca2+ channels in nerve cell bodies of corpus striatum. Journal of neurochemistry. 1986; 47:1552–1557. [PubMed: 2428938]

Satin J, Schroder EA, Crump SM. L-type calcium channel auto-regulation of transcription. Cell calcium. 2011; 49:306–313. [PubMed: 21295347]

Schroder E, Magyar J, Burgess D, Andres D, Satin J. Chronic verapamil treatment remodels ICa,L in mouse ventricle. American journal of physiology. Heart and circulatory physiology. 2007; 292:H1906–1916. [PubMed: 17158651]

Shen JB, Jiang B, Pappano AJ. Comparison of L-type calcium channel blockade by nifedipine and/or cadmium in guinea pig ventricular myocytes. The Journal of pharmacology and experimental therapeutics. 2000; 294:562–570. [PubMed: 10900233]

Shibasaki M, Kurokawa K, Ohkuma S. Upregulation of L-type Ca(v)1 channels in the development of psychological dependence. Synapse. 2010; 64:440–444. [PubMed: 20169575]

Suwanjang W, Phansuwan-Pujito P, Govitrapong P, Chetsawang B. The protective effect of melatonin on methamphetamine-induced calpain-dependent death pathway in human neuroblastoma SH-SY5Y cultured cells. Journal of pineal research. 2010; 48:94–101. [PubMed: 20050990]

Thayer SA, Murphy SN, Miller RJ. Widespread distribution of dihydropyridine-sensitive calcium channels in the central nervous system. Molecular pharmacology. 1986; 30:505–509. [PubMed: 2431262]

Thiriet N, Jayanthi S, McCoy M, Ladenheim B, Lud Cadet J. Methamphetamine increases expression of the apoptotic c-myc and L-myc genes in the mouse brain. Brain research. Molecular brain research. 2001; 90:202–204. [PubMed: 11406298]

Tippens AL, Pare JF, Langwieser N, Moosmang S, Milner TA, Smith Y, Lee A. Ultrastructural evidence for pre- and postsynaptic localization of Cav1.2 L-type Ca2+ channels in the rat hippocampus. The Journal of comparative neurology. 2008; 506:569–583. [PubMed: 18067152]

Tsai CT, Wang DL, Chen WP, et al. Angiotensin II increases expression of alpha1C subunit of L-type calcium channel through a reactive oxygen species and cAMP response element-binding protein-dependent pathway in HL-1 myocytes. Circulation research. 2007; 100:1476–1485. [PubMed: 17463319]

Uramura K, Yada T, Muroya S, Shioda S, Shiratani T, Takigawa M. Methamphetamine induces cytosolic Ca2+ oscillations in the VTA dopamine neurons. Neuroreport. 2000; 11:1057–1061. [PubMed: 10790882]

Vezina P, Queen AL. Induction of locomotor sensitization by amphetamine requires the activation of NMDA receptors in the rat ventral tegmental area. Psychopharmacology. 2000; 151:184–191. [PubMed: 10972464]

White FJ, Kalivas PW. Neuroadaptations involved in amphetamine and cocaine addiction. Drug and alcohol dependence. 1998; 51:141–153. [PubMed: 9716936]

Wolf ME. The role of excitatory amino acids in behavioral sensitization to psychomotor stimulants. Progress in neurobiology. 1998; 54:679–720. [PubMed: 9560846]

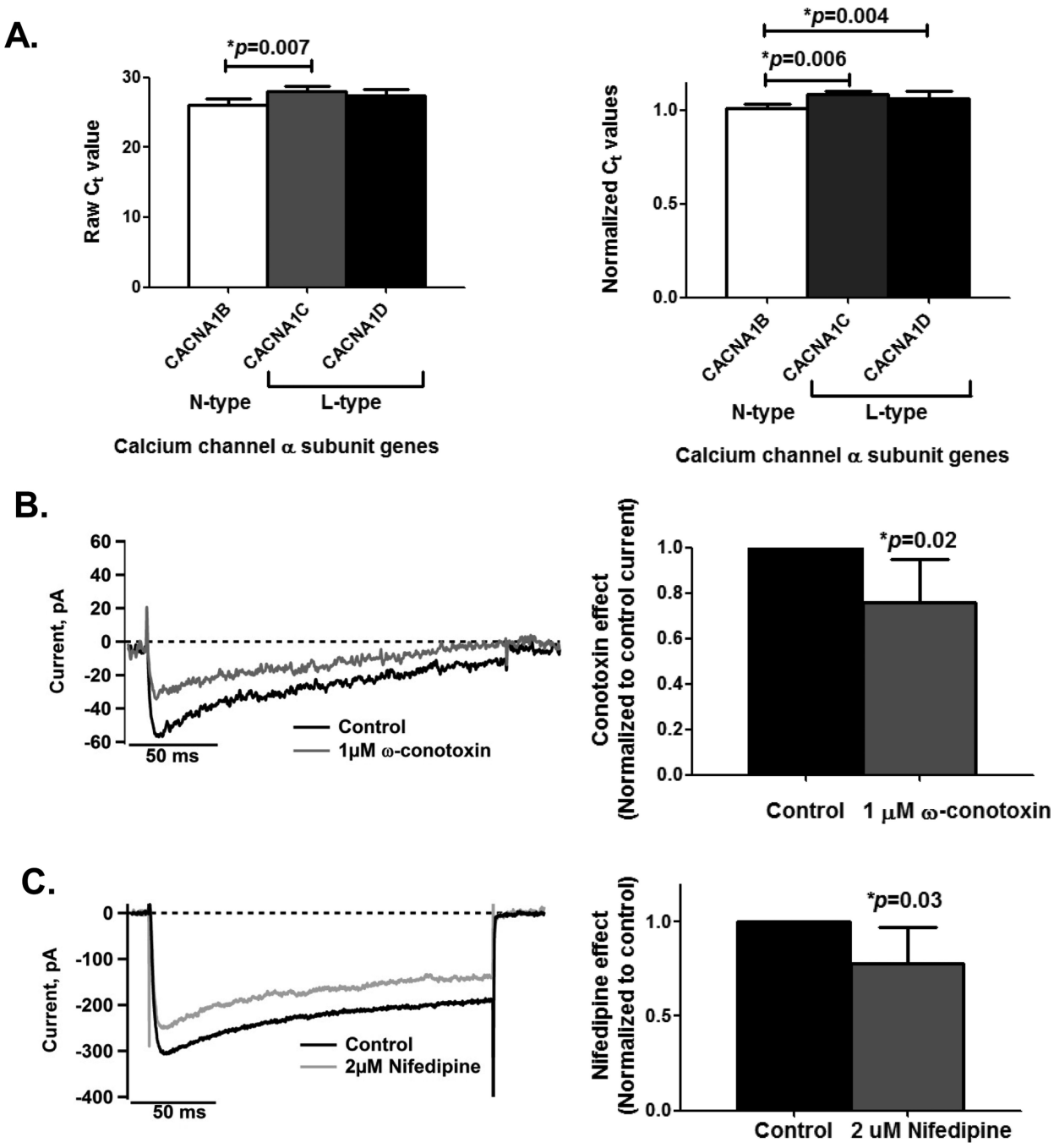


**Figure 1. L- and N-type voltage-gated $Ca^{2+}$ channels are expressed in the differentiated human cell line SH-SY5Y**

*A.* qPCR analyses indicate that *CACNA1B* gene (n=5), which encodes for the N-type $Ca^{2+}$ channel, has lower expression levels than L-type $Ca^{2+}$ channel genes, *CACNA1C* (n=5) and *CACNA1D* (n=5) (Normalized Ct ANOVA, $p$=0.005). The Ct values from qPCR raw measurements (left panel) and the normalized Ct values (right panel) are shown. Note that Ct values are inversely proportional to the RNA levels in the samples. Total RNA was extracted from harvested cells 48 hours after plating. Group means were statistically compared using 1-way ANOVA with Bonferroni's Multiple Comparison Test.

*B*. Whole-cell patch clamp recordings from a representative cell (left panel) and from a group of cells (n=5; right panel) show partial suppression of inward $Ca^{2+}$ currents when cells are exposed to 1μM ω-conotoxin solution, inhibiting N-type $Ca^{2+}$ channels by 24.4±19SD% (paired *t*-test, p=0.02). Current inhibition at this non-saturating dose was maximal within 3-5 minutes after application of toxin.

*C*. As in 1B, treatment with 2μM nifedipine, a selective blocker for L-type $Ca^{2+}$ channels, also shows inhibition of inward $Ca^{2+}$ currents by 22±19SD% (paired *t*-test, p=0.03) based on whole-cell recordings from a representative cell (left panel) and from a group of cells (n=6; right panel). Currents at this non-saturating dose were suppressed within 1-2 minutes after application of nifedipine.

In 1B and 1C, inward currents are evoked by a depolarizing step to +30mV for 200 ms from a holding potential of -90mV. Group comparisons are from cells each having been exposed to both control solution and a solution supplemented with one of the blockers. Control solution is selective for recording of $Ca^{2+}$ currents (see Methods).

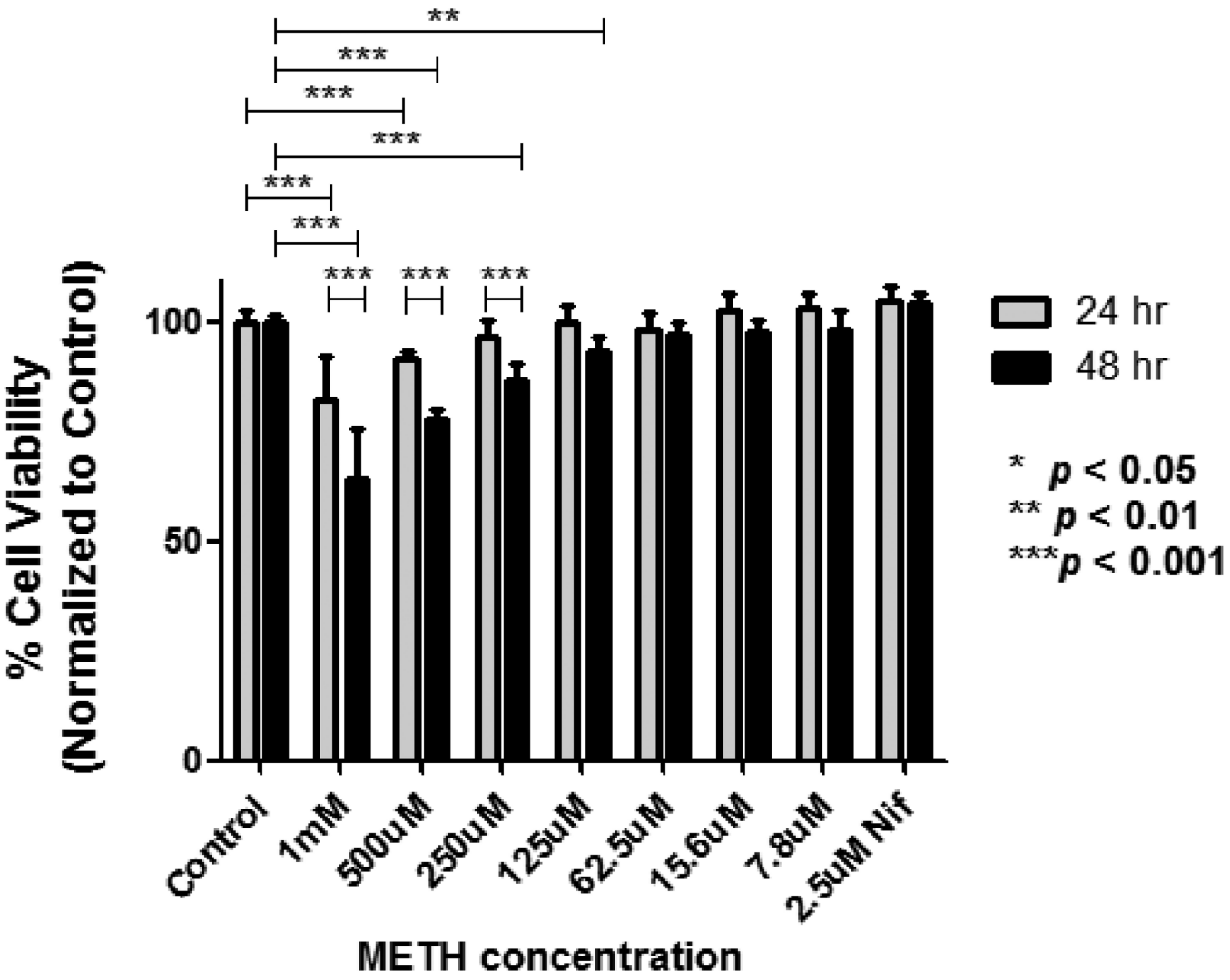


**Figure 2.**

Dose-dependent effects of METH on cell viability. SH-SY5Y cells were treated with different concentrations of METH, ranging from 7.8μM to 1.0mM, for 24 hrs (n=8 wells for each specified concentration) and 48 hrs (n=8 wells for each specified concentration). Shown also (for the far right bars) are the effects of 2.5μM nifedipine alone at the indicated exposure times. 2-way ANOVA with Bonferroni post-tests was used to compare group means between 24hr and 48hr treatments.

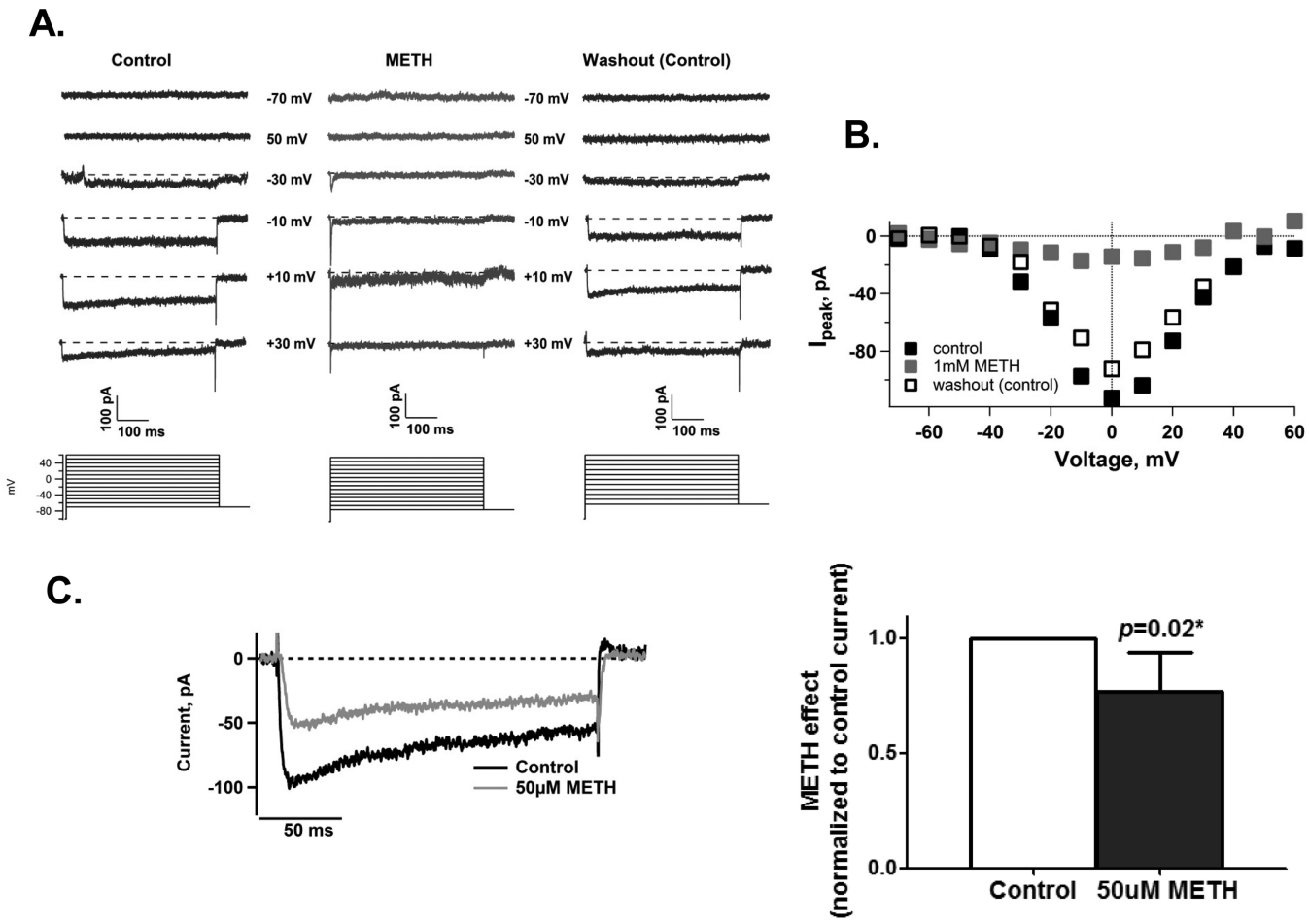


**Figure 3. METH reversibly inhibits $Ca^{2+}$ channels**

*A*. Whole-cell patch clamp recordings of a representative cell under control solution (*left panel*), 1mM METH (*middle panel*), then under washout with control solution (*right panel*). Inward currents were evoked by a family of depolarizing voltage steps ranging from -70 to +60mV for 500ms with 10mV increments from a holding potential of -70mV. Selected voltage steps are shown for clarity and ease of comparison and barium ions were used as charge carriers. Note the suppression of inward currents in response to METH and the return of these currents upon washout.

B. I-V curve of the families of inward currents for the cell shown in 3A.

C. A physiological concentration of METH (50μM) also reduces inward $Ca^{2+}$ currents as shown by whole-cell recordings from a representative cell (left panel; METH trace recorded in less than 5 min after METH exposure) and from cells exposed to control solutions and then to 50μM METH solutions (right panel: METH reduced $Ca^{2+}$ currents by 24 ± 17SD%, n=5 cells, paired *t*-test $p$=0.02). As in Figure 1, using the same depolarizing procedure, group comparisons were from patch clamp recordings of cells each having survived patch clamp recording in both control and METH-containing solutions.

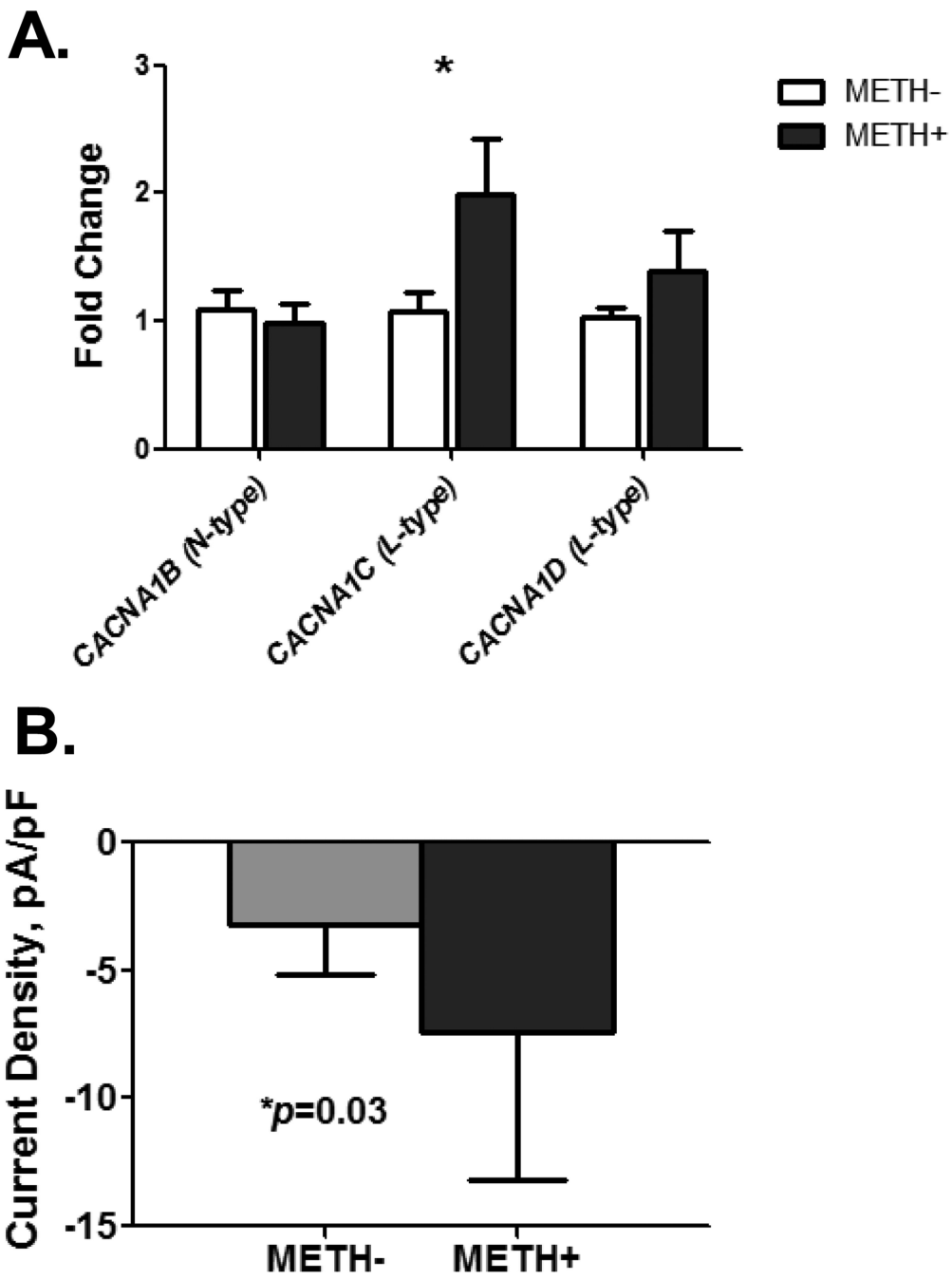


**Figure 4. The long-term effect of METH involves upregulation of L-type $Ca^{2+}$ channels**

*A.* Exposure to 50μM METH for 48 hours upregulates the expression of *CACNA1C* (n=6-10, unpaired *t*-test $p$=0.049) but not *CACNA1B* (n=6-10) and *CACNA1D* (n=6-10). qPCR analysis is used to measure fold change in response to METH treatment. Values for each gene are normalized to the value for the corresponding gene of untreated-cells.

*B.* Treatment of cells with 50μM METH for 20 min significantly increased inward whole-cell current density (n=5 METH-, n=11 METH+, $p$=0.05 by unpaired *t*-test with Welch's correction) as early as 3 hrs post-treatment. Inward currents are induced by a depolarizing

step to +20mV for 200 ms from the holding potential of -70mV. Barium ions were used as charge carriers to increase the signal-to-noise ratio.

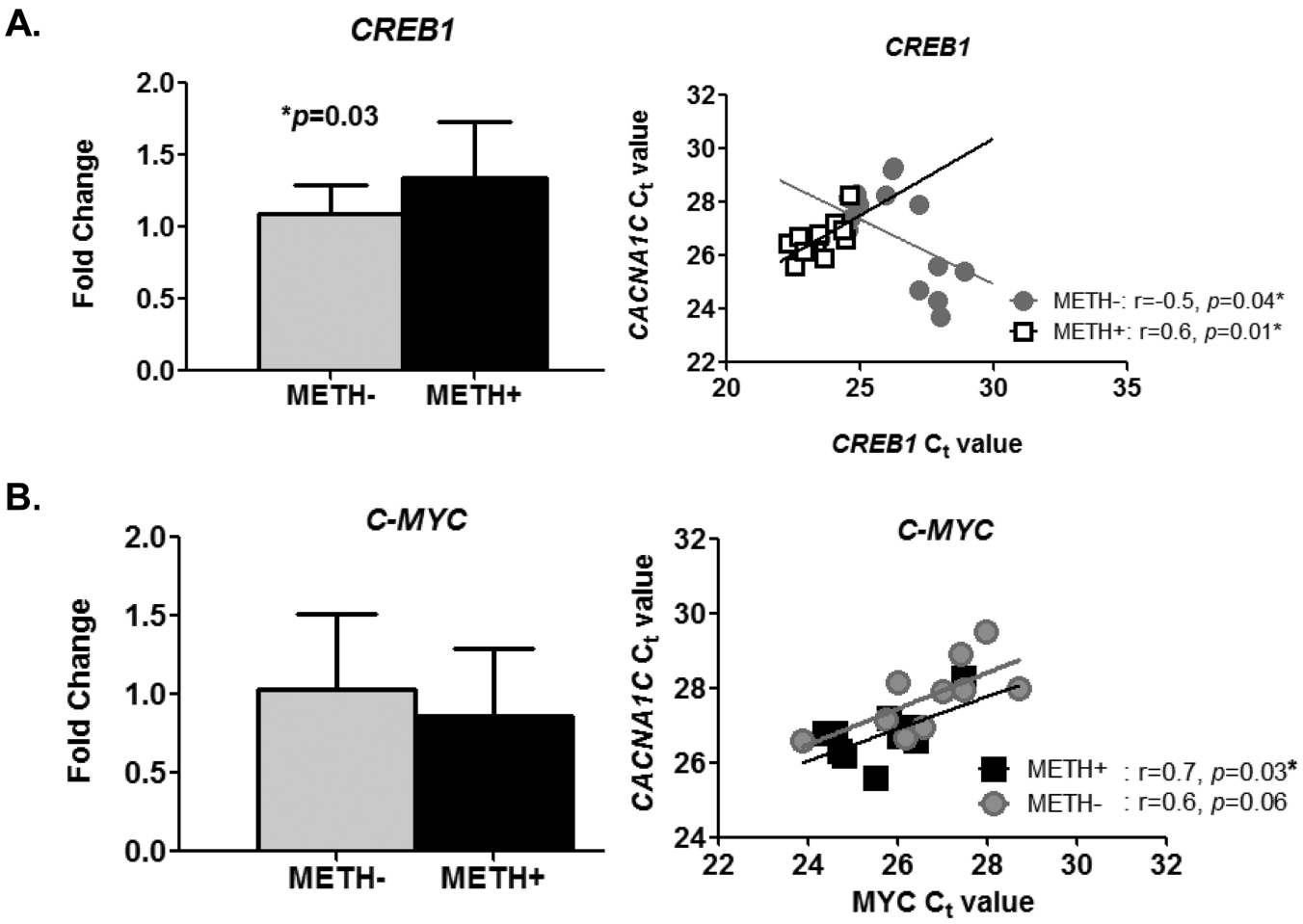


**Figure 5. Relationship between *CACNA1C* and *CREB1* or *C-MYC* expression in METH-treated and untreated cells after 48 hr drug treatment**

*A. CREB1* expression is significantly higher ($p$=0.03 by unpaired $t$-test) in METH-treated cells (n=13) compared to untreated cells (n=13) (left panel). *CREB1* expression levels are positively correlated to *CACNA1C* expression levels in METH-treated cells but inversely correlated in untreated cells (right panel: ANCOVA, $p$=0.04).

B. Expression levels of *MYC* gene in METH-treated cells (n=14) is not significantly different ($p$=0.2 by unpaired $t$-test) than those found in untreated cells (n=14) (left panel). The right panel shows the scatter plot when data was stratified according to drug treatment; *CACNA1C* expression is significantly correlated with the expression levels of *C-MYC* genes (overall r=0.7, p=0.0002). However, the slopes of METH and untreated cells were not different from each other (ANCOVA $p$=0.5).

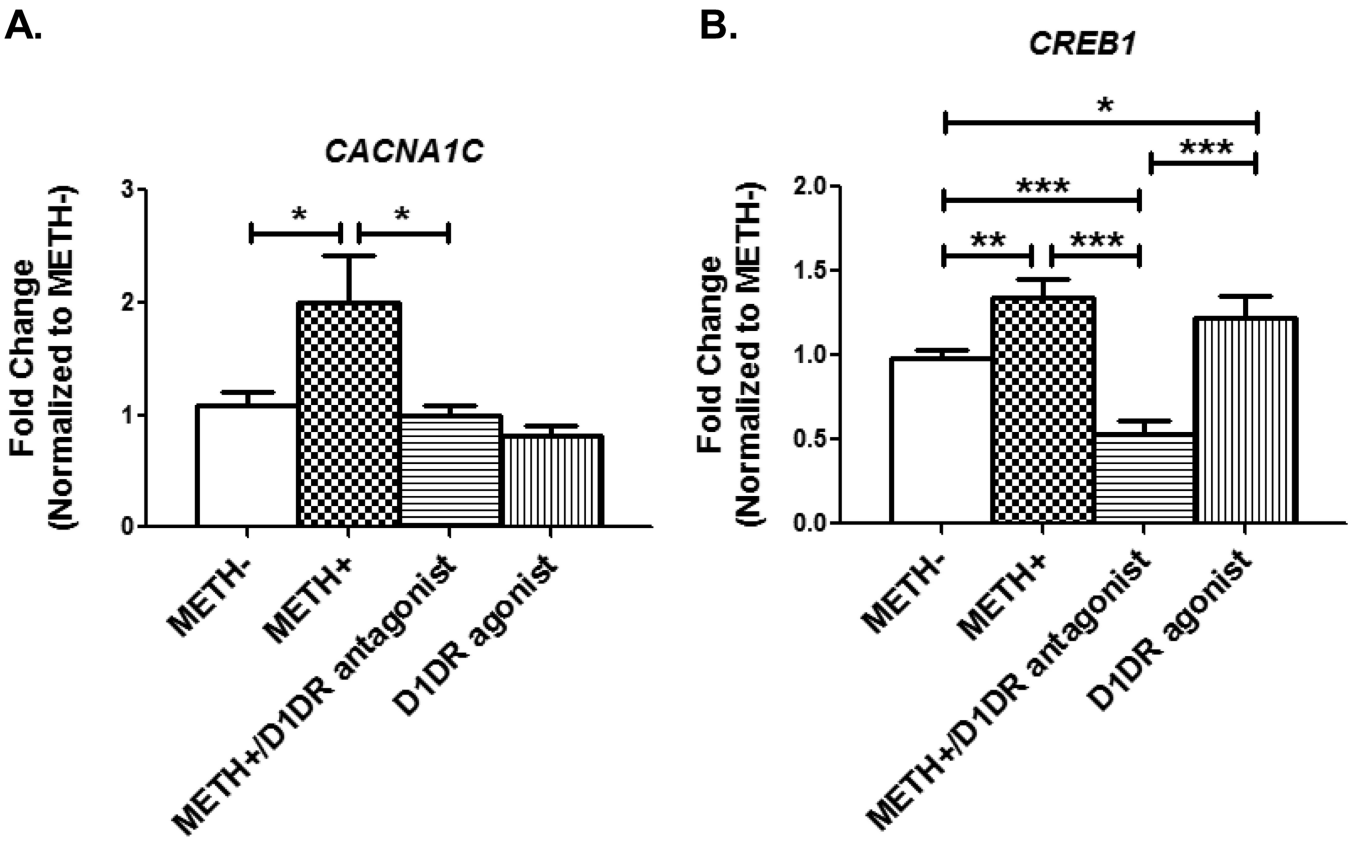


**Figure 6. The dopamine D1 receptor signaling system affects CREB1 expression**

A. Treatment of cells with 50μM METH upregulates *CACNA1C* expression (METH- vs METH+, $p$=0.02). Blocking the dopamine D1 receptors with 10μM SCH 23390 in the presence of METH reduces *CACNA1C* expression (METH+ vs METH+/D1DR antagonist, $p$=0.05) to levels comparable to untreated cells (METH- vs METH+/D1DR antagonist, $p$=0.35). Activating the dopamine D1 receptors with the agonist SKF 82958 (10μM; 4$^{th}$ bar) has no effect on calcium channel expression ($p$=0.15). Shown are data from untreated cells (METH-, n=14), cells treated with 50μM METH for ≥20 min up (METH+, n=10), cells pre-incubated with 10μM SCH 23390 for 50 min and then subsequently incubated with 50μM METH for 20min (METH+/D1DR antagonist, n=6), and cells incubated with 10μM SKF 82958 (D1DR agonist, n=4) for 20 min. Group means were compared using 1-way ANOVA with Bonferroni's Multiple Comparison Test.

B. Cells treated with the dopamine D1 receptor antagonist SCH 23390 and METH (METH +/D1DR antagonist, n=6) show lower levels of *CREB1* expression compared to untreated cells (METH-, n=12;$p$=0.0001), METH-treated cells (METH+, n=13, $p$<0.0001), and D1 receptor agonist-treated cells (D1DR agonist, n=4, $p$=0.0007). Group means were compared using 1-way ANOVA with Bonferroni's Multiple Comparison Test. Treatment regimens for SCH 23390, SKF 82958 and METH are the same as those described in 6A.

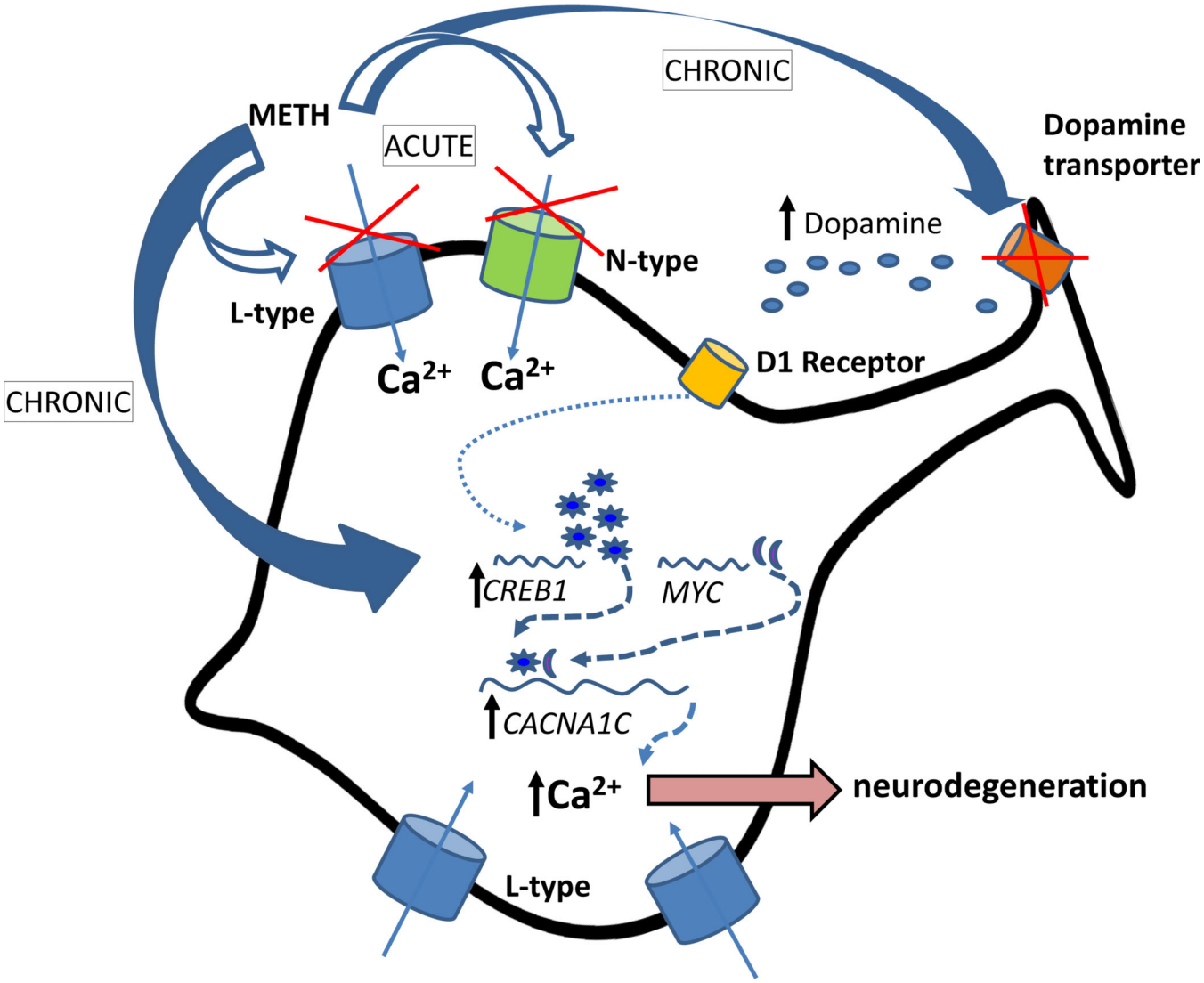


**Figure 7.**
Schematic illustration of proposed mechanisms.